Journal of Plant Protection Research eISSN 1899-007X

ORIGINAL ARTICLE

# Smart sprayer for weed control using an object detection algorithm (yolov5)

Ameer H. Al-Ahmadi, Alaa K. Subr*

Department of Agricultural Machines and Equipment, College of Agricultural Engineering Sciences, University of Baghdad, Baghdad, Iraq

**DOI: 10.24425/jppr.2025.155782**

Received: April 11, 2024
Accepted: June 24, 2024
Online publication: September 23, 2025

*Corresponding address:
alaa.kamel@coagri.uobaghdad.edu.iq

Responsible Editor:
Zbigniew Czaczyk

**Abstract**

Spraying pesticides is one of the most common procedures that is conducted to control pests. However, excessive use of these chemicals inversely affects the surrounding environments including the soil, plants, animals, and the operator itself. Therefore, researchers have been encouraged to develop robotic sprayers that can apply pesticides at variable rates as needed in the field. In this study, a remotely controlled sprayer with two modes (variable rate and constant rate applications) was developed and evaluated for some spray characteristics and application accuracy metrics when controlling weeds at two travel speeds. The variable rate mode resulted in a high precision, recall, and accuracy in detecting weed and applying herbicide that was 90%, 100%, and 94%, respectively. Moreover, the spray coverage, droplet density, and the deposition on weed using the variable rate mode were 34.16%, 127.64 deposites · $cm^{-2}$, and 7.67 µl · $cm^{-2}$, respectively. The result also revealed that the spray coverage, droplet density, and the deposition were less sensitive to the travel speed when adopting the variable rate mode compared to the constant rate mode.

**Keywords:** agricultural robot, precision agriculture, smart spraying, YOLOv5, weed control

## Introduction

Weed is referred to as any undesired plant that usually grows non uniformly in the field (Partel *et al.* 2019a; Farooque *et al.* 2023) along with the main crop and competes with the main crop for soil nutrients, irrigation water, and even sunlight that leads to exorbitant losses (Idziak *et al.* 2022; Shah *et al.* 2021) which may exceed that induced by other pests (Sujaritha *et al.* 2017; Dian Bah *et al.* 2018). Weeds negatively influence the quality characteristics of the crops (Al-Chalabi and Hammood 2016a). In addition, weeds represent suitable environment to develop pests and diseases (Al-khazali and Shati 2016; Kulkarni *et al.* 2019; Subeesh *et al.* 2022).

Spraying herbicides pre-emergence or post-emergence (Al-khazali and Shati 2016; Veisi *et al.* 2020; Idziak *et al.* 2022) is the most common procedure followed to control weeds. This procedure is usually performed uniformly on the field regardless of the actual distribution of weeds (Hussain *et al.* 2021a; Urmashev *et al.* 2021). Although this procedure ensures a high efficacy of controlling weeds, its excessive use increases costs, health issues for those who are exposed to the chemicals (Shah *et al.* 2021), contamination of surrounding environment including air, water, soil, animals, and vegetation (Zhu *et al.* 2017; Kulkarni *et al.* 2019), increasing the weed resistance to chemicals applied (Adamczewski *et al.* 2019), and destroying some of the desired plant by the chemicals applied (Aravind *et al.* 2016) or exposing the main crop to the toxic effect of the herbicide used (Pannacci and Bartolini 2018). These risks aggravate much more when applying chemicals inside greenhouses (Subeesh *et al.* 2022).

Uniform spraying may be preferred when there is not a significant variation in weeds or diseases distribution in the field, whereas variable rate spraying may be desired when the distribution of weeds and diseases is patchy in the field (Villette *et al.* 2021; Farooque *et al.* 2023).

Deep learning is a part of artificial intelligence (Shah *et al.* 2021) and has appeared as a promising technique to deal with enormous dataset for classification and detection purposes (Chandel *et al.* 2021) by recognizing similarities and differences within the data using proper algorithms without required predefinitions (Shah *et al.* 2021).

Kulkarni *et al.* (2019) proposed a convolutional neural network to distinguish weed from crop based on Watershed Image segmentation Algorithm that achieved an average accuracy of 85%. They recommended that a drone or a robot sprayer can be accompanied by this algorithm to spray herbicides as needed in the field.

Partel *et al.* (2019a) developed a smart sprayer for weed control based on a deep neural network, namely YOLOv3. They trained the tiny YOLOv3 and YOLOv3 using 1000 images of the studied artificial and real plants and weeds and compared them to Faster R-CNN (Resnet50), Faster R-CNN (Resnet101). It was found that Faster R-CNN (Resnet50) achieved the best precision and recall, whereas the YOLOv3 excelled at the processing time.

Urmashev *et al.* (2021) compared the performance of three machine learning algorithms and a convolution neural network to distinguish four weed species. The machine learning algorithm studied included K-Nearest Neighbor, Random Forest, and Decision Tree, whereas the convolution neural network was YOLOv5. The performance of these algorithms was evaluated based on several metrics such as false positive rate, false negative rate, precision, recall, and accuracy. The detection accuracy of all the studied algorithms ranged from 80% to 92%.

This research aimed to develop a smart sprayer using inexpensive commercially available materials that applies herbicide (tap water was used for safety consideration) at variable rate as needed, evaluation of the detection and identification system, and to compare some spraying parameters with the constant variable mode.

## Materials and Methods

### The platform

A four-wheel small platform (Fig. 1) was designed with a length, width, and clearance above the ground of 80, 45, 30 cm, respectively to be able to work in between the crop rows. The two rear wheels (driving wheels) were with a diameter of 28 cm, each had a DC motor (DG-168A2, working current: 24 V, unloading speed: 140 rpm). While the two front wheels were caster wheels with a diameter of 20 cm. This platform was designed to be controlled remotely by a wireless controller (MicroZone 2.4G 6CH MC6C Remote Controller). The steering system of this platform was a skidding type that depends on the differential motion between the two wheels. A 12-Volt battery was used as a power supply for the DC motors and the solenoids valves.

### Spraying system

The spraying system consisted of a commercial 16-liter backpack sprayer (Al-Chalabi and Hammood 2016a, 2016b; Al-khazali and Shati 2016; Al-Khafaji *et al.* 2023) that contained a tank, battery, pump (Table 1), and pressure regulator and operated electrically. In addition, the spraying system contained a return line with a nozzle, pressure gauge to monitor the pressure

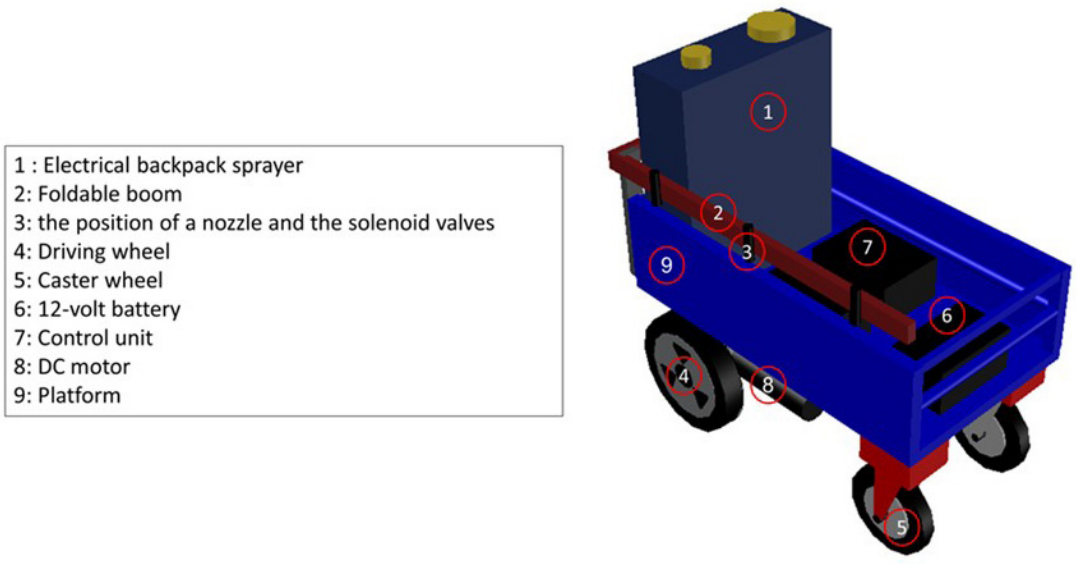


**Fig. 1.** The scheme of the developed sprayer (drawn by AutoCAD 2017)

**Table 1.** Sprayer pump specifications

| Specification | Description |
|---|---|
| Max pressure | 4.8 |
| Open flow | 3.1 l · min$^{-1}$ |
| Voltage | 12 |
| Max current | 2 |

**Table 2**. Nozzle specifications

| Specification | Description |
|---|---|
| Model | TeeJet |
| Type | air Blast disc-core type full cone |
| Material | stainless steel |
| Working pressure | 1.34–20 |
| Flow rate @ 2 bar | 0.64 @ 2 |
| Spray angle | 65° |

within the system, filters to purify the spray solution, three 12-Volt normally closed solenoid valves to control the nozzle action. Three disc-core nozzles (that produce full cone pattern were used in the study. This type of nozzles has a narrow spraying area (Marangoni Junior and da Costa Ferreira 2019) which make it qualified for spot spraying purposes. Although, even flat fan nozzles may reduce the potential of bad coverage on the boundaries of the spray, we recommended using the full cone nozzle that may be better for spot spraying.

## Control unit

The control unit consisted of an Arduino mega microcontroller board and Microzone MC6C 6 Channel Radio Set 2.4GHz transmitter and receiver as steering controller to control the speed and the steering of the vehicle by controlling the DC motors (Table 3) via PWM driver board (Table 4), a camera (Table 5), relays. Additionally, A Raspberry Pi 4 model B-8 Gb was

**Table 3**. DC motor specifications

| Specification | Description |
|---|---|
| Model | DG-168A2 |
| Unloading voltage | 24 |
| Unloading current | up to 4.5 |
| Unloading maximum speed | 135 |
| Output power | 150 |
| Gear ratio | 26.25 |
| Gear motor rated torque | 11.3 |
| Weight | 4.63 |

**Table 4.** PWM driver board specifications

| Specification | Description |
|---|---|
| Input voltage | 6–27 |
| Maximum current | 43 |
| Input level | 3.3–5 |

**Table 5.** Camera Specifications

| Specification | Description |
|---|---|
| Dimension | |
| Frame rate | 29.6 |
| Horizontal field of view | |
| Vertical field of view | |

used as computer board with a set of general-purpose input/output (GPIO) pins via which actuators can be controlled (Raspberry Pi Foundation, Cambridge, UK) (Coleman *et al.* 2022) associated with An Edge TPU coprocessor (Coral USB accelerator) to accelerate the performance of the Raspberry Pi to obtain a reasonable inference time

A python script was developed to utilize the YOLOv5s model for weed detection. This script divided the image obtained by the camera into three vertical equivalent sections. Each vertical section controlled one of three lines (Coleman *et al.* 2022) and was related to a solenoid valve and a nozzle thus one camera covered three lines. To best our knowledge this method of dividing a single camera into several zones and controlling each zone separately is a novel method that can increase the precision of applying herbicides as needed in the field.

A horizontal threshold can be adjusted to focus on the weeds that exist just under the camera to avoid pre or post spraying. In our case, the solenoid was programed to open when the weed is detected at the lower third of the image to avoid the pre-spraying.

The location of the predicted plant including the pepper and the weed center was calculated based on the bounding box coordinates assuming that the plant is symmetrical radially (Shah *et al.* 2021). Therefore, the center coordinates of a detected plant were calculated by the following equations 1:

$$c_x = \frac{x_1 + x_2}{2}, \qquad c_y = \frac{y_1 + y_2}{2},$$

where:

$c_x$, $c_y$ – the $x$, $y$ coordinate of the predicted plant center;

$x_1$, $y_1$ – the $x$, $y$ coordinate of the upper left point of the predicted bounding box;

$x_2$ – the $x$, $y$ coordinate of the lower right point of the predicted bounding box.

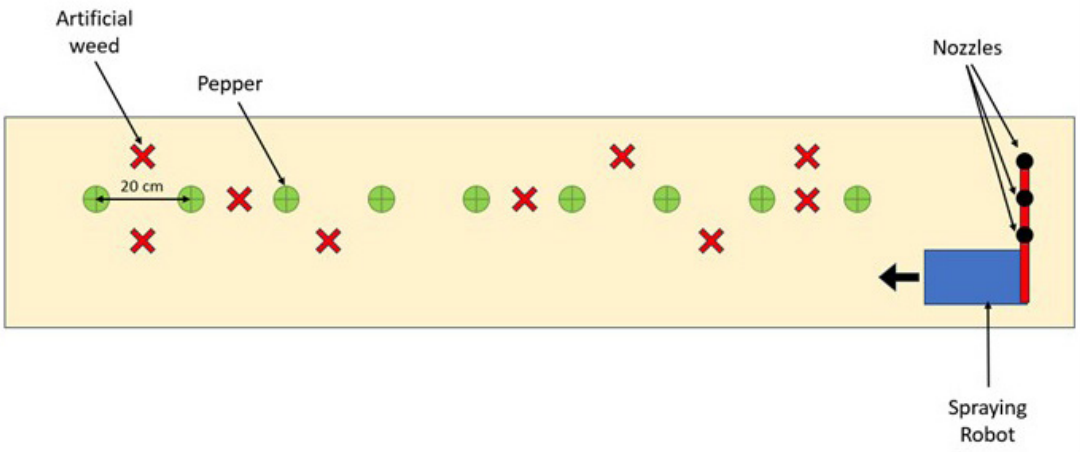


**Fig. 2.** Shows an example of the arrangement of a treatment line

## Field experiment

This experiment investigated the effect of two spraying systems including a developed remotely controlled variable-rate sprayer (VRS), and a remotely controlled constant-rate sprayer (CRS), two forward speeds including 2 km · h$^{-1}$, and 3 km · h$^{-1}$, and two types of vegetation including green pepper (*Capsicum annuum*) seedlings and an artificial weed. The operation pressure was fixed at 3 bars. Thus, this experiment was arranged as a completely randomized design (CRD) and was analyzed as a factorial experiment with three factors under controlled environment.

The experiment was performed in a paved courtyard in the college of Agricultural Engineering Sciences – University of Baghdad (33°16'2.68"N, 44°22'46.66"E) in June 2023 from 7:00 am to 11:00 am. The temperature ranged from 26 to 33, the relative humidity was 20%, and the wind was north-western with a speed ranged from 8 to 12 km · h$^{-1}$. For each treatment, a strip of nine 1-liter containers (Zhu *et al.* 2017) spaced at 50 cm and each of them contained green pepper seedlings at establishment growth stage about 4 weeks after planting along with nine artificial weeds that were randomly distributed on the right, left, inline of the pepper containers (Fig. 2) which led to a weed density of 2 weeds per square meter.

Since there were two remotely controlled sprayers, it requires two different booms. The boom of the CRS sprayer consisted of three full cone nozzles with flow rate of 0.4 l · min$^{-1}$ and fan angle of 45° with 25 cm between each two successive nozzles. The nozzles' tips were 30 cm above the ground. All the nozzles were mounted on wooden timber. On the other hand, the boom of VRS sprayer was similar to that of the CRS but it has a 12-Volt normally closed ½" DC12V solenoid valves before each nozzle that can activate or deactivate the spray flow based on the presence or absence of the weeds whose locations are within the effect zone of that nozzle (Fig. 3).

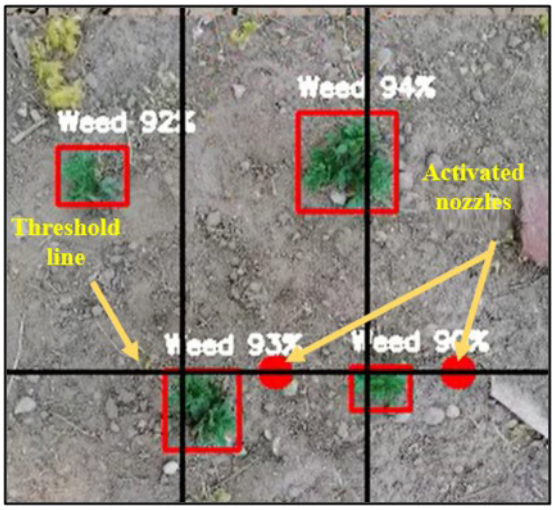


**Fig. 3.** Shows the threshold line and how the nozzles (illustrated in red circles) is work when detecting artificial weeds

In relative the application rate, for CRS it was 600 and 400 l · ha$^{-1}$ for the speed of 2 and 3 km · h$^{-1}$, respectively considering the following equation the spray swath of 0.75 m, the travel speed of 2 and 3 km · h$^{-1}$, and the nozzle flow rate of 0.5 l · min$^{-1}$. Equation 2:

$$R_A = \frac{N \times C \times Q}{S \times L}$$

where:
$R_A$ – application rate (l · ha$^{-1}$);
$N$ – number of nozzless;
$Q$ – flow rate per nozzle (l · m$^{-1}$);
$S$ – forward split (km · h$^{-1}$);
$L$ – length of the boom (m);
$C$ – conversion factor equals to 600.

However, the above equation did not work for the VRS mode since the flow rate of the nozzles is not continuous and we suggest that the application rate for VRS can be calculated based on the following equation which requires a pre-knowledge about the flow rate of

the nozzle used ($Q$) that can be calculated on the field, the total time for opening the nozzles ($t$) that can be recorded by the software used, and the area sprayed per unit time ($A$) that can be calculated multiplying the spraying swath by the travel speed. Therefore, the average application for the VRS would be 27.7 and 18.5 $l \cdot ha^{-1}$ for the travel speed of 2 and 3 $km \cdot h^{-1}$, and an average time for opening the nozzle of 500 ms.
Equation 3:

$$R_A = \frac{Q \times t \times 10^4}{A}$$

It should be mentioning that the amount of spray on a single weed using VRS mode will not differ from that of CRS since the flow rate of the nozzle and the travel speed are fixed the only different between the VRS and the CRS is that the nozzle is continuously opened in CRS while it is opened only when a weed is detected under its region of effectiveness.

## Estimating spray parameters

Spray parameters including the spray coverage (Spray coverage is a spray attribute that reflects the percentage of target area covered with stains relative to the total area (Cunha *et al.* 2012; Ferguson *et al.* 2016; Zhang *et al.* 2016; Subr *et al.* 2020; Marwan and Subr 2022) and droplet density (Droplet density is another spray parameter that refers to the number of droplets per unit area (Zhang *et al.* 2016; Marwan and Subr 2022) were estimated using water sensitive papers (WSPs) that were placed at each plant and artificial weed and were collected after about 1 minute after each treatment to let them dry adequately before they were collected using a plastic tweezer and placed in a transparent self-adhesive nylon bag. Then, the WSPs were scanned by a scanner (MFC-J480DW, Brother Corporation) at a resolution of 600 dpi (Subr *et al.* 2020; Marwan and Subr 2022).

DepositScan software (USDA, Wooster, OH, USA) was used to analyze the scanned images to estimate the parameters (Zhu *et al.* 2011; Cunha *et al.* 2012). Tap water was used as a spray solution. However, it should be mentioned that the spray parameters measurement may differ with the quality of water or when using a surfactant (Parafiniuk *et al.* 2015, 2017; Subr *et al.* 2020a ; Milanowski *et al.* 2022).

## Dataset preparation for training the convolution neural network

A dataset comprised of 849 images was used for training the model. This dataset consists of 435 images for green pepper (*Capsicum annuum*) that were grown in the Horticultural Station, the Ministry of Agriculture, Baghdad, Iraq (33°19'21.77"N, 44°14'12.69"E), and 414 images for artificial weed. These images were captured under different positions and angles at height ranged from 60 to 80 cm above the ground for each plant from 10:00 am to 1:00 pm on April 5, 2023, when the pepper plants were at early growth stage (eight weeks) via the main camera of a Huawei P30 Lite smartphone using an aspect ratio of 1:1 to obtain square RGB images with 2992 × 2992 × 3 dimension. The images were taken at early growth stage to avoid the dense vegetation and overlap of contiguous plants that are considered a challenge for plant and weed discrimination (Bakhshipour and Jafari 2018).

## YOLOv5 as convolution neural network

YOLOv5 is a version of deep learning algorithms namely "You Only Lock Once" that is used for classification, segmentation, or object detection. It is preferable for its high accuracy small inference time that made it eligible for real time detection tasks. YOLOv5 differs from the previous versions of YOLO in that it utilizes the PyTorch framework – that is more popular for machine learning applications – rather than Darknet, it is less complex, and requires less inference time comparing to the previous versions (Hussain *et al.* 2021b).

This network as explained by (Urmashev *et al.* 2021) is composed of three main parts: Backbone, Neck, and Head. As illustrated in (Anon n.d.), the Backbone part is composed of a number of convolution, normalization, and activation layers that are responsible for feature extraction and image downsampling. The Neck part processes the feature outputs obtained from the Backbone part and producing feature maps at different scale to enhance the model generalization, then transmitting them to the Head part which creates the final detection information including the coordinates, height and width of the predicted bounding boxes, the confidence score, and the predicted class for each predicted bounding box (Anon n.d.).

Python is considered a promising programming language for robotic task due to its simplicity and the availability of its resources and libraries (Shah *et al.* 2021), therefore it was used for processing the images, training the convolution neural network algorithm (YOLOv5s), and to create a scratch for detecting weeds and applying pesticides. The images were resized using resize method of the OpenCV library in a python script to get 416 × 416 images. This step was required to reduce the resolution of the images to decrease the time cost for training the model and then detecting objects within an image.

Then, the images were labelled for pepper and weeds using Labelimg tool V 1.8.6 (Shah *et al.* 2021; Wang *et al.* 2022) using YOLO format that compatible with YOLOv5 model that was used as a pretrained model later. Therefore, for each image an associated txt

file was generated as an annotation file which contains information about the class id, the x and y coordinates of the bounding box center, and the width and height of the bounding box for each object in the image.

After labeling, the dataset (including the images and their associated annotation files) was augmented using the roboflow platform (https://roboflow.com/) using horizontal flip, vertical flip, clockwise 90° rotation, counter-clockwise 90° rotation, rotation between –15 and +15, ±15 horizontal shear, ±15 vertical shear, saturation between –15 and +15, brightness between –20 and +20, exposure between –10 and +10, blur up to 1.25 px, and noise up to 4% of pixels. This augmentation results in a dataset of 2112 images. This dataset was split into 90% for training (1900 images), 8% for validation (170 images), and 2% for testing (42 images). The training is performed using a laptop (Lenovo, ideapadGAMING, 11th Gen Intel(R) Core(TM) i7-11370H @ 3.30GHz, 16 GB RAM).

The hyperparameter adopted for this training are shown in (Table 6). The weight file with an extension of (.pt) was converted into a file of (.tflite) extension using an image size of  to be utilized on the Raspberry pi 4 model B – 8 GB associated with a Google Edge TPU ML accelerator to enhance the Raspberry pi performance especially the speed of processing data.

**Table 6.** Hyperparameters for training the model

| Hyperparameter | Value |
|---|---|
| Image size | 416 |
| Epochs | 100 |
| Batch size | 16 |
| Learning rate | 0.01 |
| Momentum | 0.937 |
| Optimizer | stochastic gradient descent (SGD) |

## Statistical analysis

### Spray parameters

Data obtained from the DepositScan software were analyzed via three-way analysis of variance (ANOVA) using Origin software (Origin, Version 2018. Origin -Lab Corporation, Northampton, MA, USA) to examine the null hypothesis that the means of all groups in each type of sprayer, the speed, and their interactions are equal. The Fisher's least significant difference (LSD) test was used as a multiple comparison test when the null hypothesis was rejected. All analyses were performed at the 0.05 level of significance.

### Prediction and herbicide application parameters

The model was evaluated based on the values obtained after training the model including the precision, recall, mAP@50, and F1-score. Moreover, the precision (Equation 4), recall (Equation 5) (Partel *et al.* 2019b; Konar *et al.* 2020; Urmashev *et al.* 2021; Al-Mahmood *et al.* 2022; Ghadi and Salman 2022; Subeesh *et al.* 2022; Wang *et al.* 2022; Farooque *et al.* 2023), accuracy (Equation 6) (Urmashev *et al.* 2021; Ghadi and Salman 2022; Nyarko *et al.* 2023), and error rate (Equation 7) (Hussain *et al.* 2021a) were calculated on the field based on the true positives (the number of weeds that were correctly classified as weeds), true negatives (the number of pepper plants that were correctly classified as non-weeds, false positives (the number of pepper plants that were incorrectly classified as weeds), false negatives (the number of weeds that were incorrectly classified as non-weeds). Please, see the table below for the parameters' references.

Equation 4:

$$\text{Precision} = \frac{TP}{TP+FP}$$

Equation 5:

$$\text{Recall} = \frac{TP}{TP+FN}$$

Equation 6:

$$\text{Accuracy} = \frac{TP+TN}{TP+TN+FP+FN}$$

Equation 7:

$$\text{Error rate} = \frac{FP+FN}{FP+FN+TP+TN}$$

where: *TP* – true positives; *TN* – true negatives; *FP* – false positives; *FN* – false negatives.

**Table 7.** References for some prediction and herbicide application parameters

| Parameter | References |
|---|---|
| Precision | Al-Mahmood *et al.*(2022); Ghadi and Salman (2022); Konar *et al.* (2020); Nyarko *et al.* (2023); Partel *et al.* (2019a); Partel *et al.* (2019b); Subeesh *et al.* (2022); Urmashev *et al.* (2021); Wang *et al.* (2022) |
| Recall | Al-Mahmood *et al.* (2022); Farooque *et al.* (2023); Ghadi and Salman (2022); Konar *et al.* (2020); Partel *et al.* (2019a); Partel *et al.* (2019b); Subeesh *et al.* (2022); Urmashev *et al.* (2021); Wang *et al.* (2022) |
| Accuracy | Ghadi and Salman (2022); Nyarko *et al.* (2023); Urmashev *et al.* (2021) |
| Error rate | Hussain *et al.* (2021b) |

The model performance is usually evaluated based on the results obtained due to training the model including the box loss (box_loss), objectness loss (obj_loss), and class loss (cls_loss). The box_loss refers to the error of predicting the center coordinates, width, and height of bounding boxes. The obj_loss refers to the error that occurred due to the ambiguity of finding an object within the investigated image. The cls_loss refers to an error that occurred when predicting an object into an incorrect class (Hussain *et al.* 2021a). It is worth mentioning that the Binary Cross Entropy is used to estimate the class and objectness losses, whereas the intersection over union loss is used to estimate the box loss (Anon n.d.). Generally, the lower the loss, the highest the model's performance.

The mean average precision (mAP) is calculated by dividing the summation of the average precisions of all the class by the number of the classes at a specific intersection over union (IOU) value such as 0.5 and from 0.5 to 0.95 for $mAP_{0.5}$ and $mAP_{0.5:0.95}$, respectively. The highest the mAP the better the model's performance.

# Results

## Spray coverage

The results revealed that there was a highly significant difference in the spray coverage ($F_{1,56}$ = 1404.4, $p \cong 0$) between the VRS and the CRS. The average spray coverage on the pepper and the weed for VRS was 17.3% compared to that for CRS that was 67.6%.

The effect of the travel speed on the spray coverage was highly significant ($F_{1,56}$ = 223.7, $p \cong 0$). The speed of 2 km · h$^{-1}$ achieved higher coverage of 52.5% compared to the speed of 3 km · h$^{-1}$ that achieved 32.4%.

The comparison between pepper and weed showed a highly significant difference ($F_{1,56}$ = 169.2, $p \cong 0$). The pepper got the lower coverage of 33.7% compared to the weed that got a coverage of 51.2%. The decrease in the coverage on pepper resulted from well distinguishing the pepper plants and not spraying them using the VRS.

The interaction between sprayer type and the travel speed showed a significant effect ($F_{1,56}$ = 19.6, $p \cong 0$). Figure 4 shows that the effect of the speed was obvious using the CRS, and the higher coverage occurred at the speed of 2 km · h$^{-1}$. Whereas the effect of the speed was not noticeable when using VRS. In other words, the spray coverage was less sensitive to the travel speed using the VRS compared to the case of using CRS.

The interaction between sprayer type and the target type showed a significant effect ($F_{1,56}$ = 146.4, $p \cong 0$). Figure 5 shows that the target type affected the spray coverage using VRS that the pepper got nearly zero coverage compared to the weed which got a coverage of 34.16%. Whereas using the CRS the coverage was 67 and 68.2% at 2 and 3 km · h$^{-1}$. This result confirms that both the target and non-target plants were sprayed uniformly using the CRS and variably based on the differentiation between the target and non-target plant using the VRS.

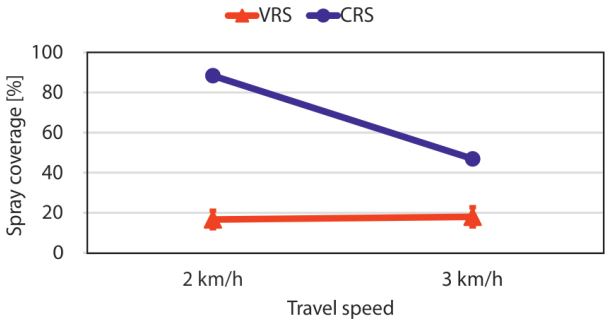


**Fig. 4.** The effect of the interaction between the sprayer type and travel speed on the coverage

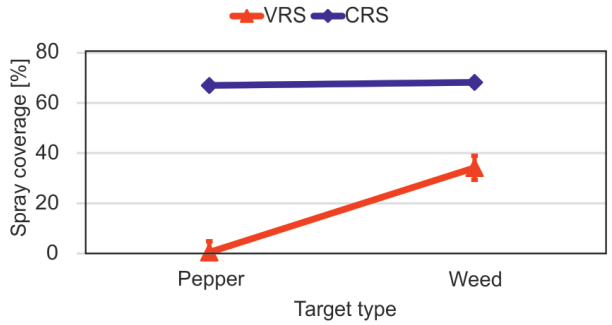


**Fig. 5.** The effect of the interaction between the sprayer type and target type on the coverage

## Droplet density

The analysis showed a highly significant effect of the sprayer type on the droplet density ($F_{1,56}$ = 314.7, $p < 10^{-2}$). The VRS achieved the higher droplet density of whereas the CRS achieved 44.7 deposit · cm$^{-2}$.

Similarly, the travel speed significantly affected the droplet density ($F_{1,56}$ = 12.1, $p < 10^{-3}$). The droplet density increased with the travel speed which was 40.8 and 70.7 deposit · cm$^{-2}$ at 2 and 3 km · h$^{-1}$ , respectively.

The target type showed a significant effect on the droplet density ($F_{1,56}$ = 10.5, $p < 10^{-8}$) where the higher value of 84.7 occurred in weed comparing to the pepper that obtained 26.8 deposit · cm$^{-2}$. It is worth mentioning that the spray density occurred on the pepper was mostly due to using the CRS.

The interaction between the sprayer type and the travel speed significantly affected the droplet density ($F_{1,56}$ = 19.6, $p < 10^{-6}$). Figure 6 illustrates that the effect of the travel speed was more noticeable with CRS

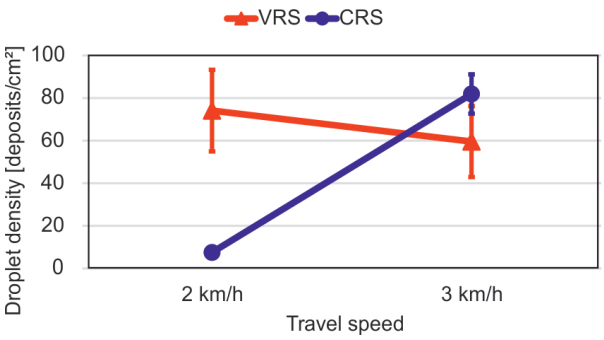


**Fig. 6.** The effect of the interaction between the sprayer type and travel speed on the droplet density

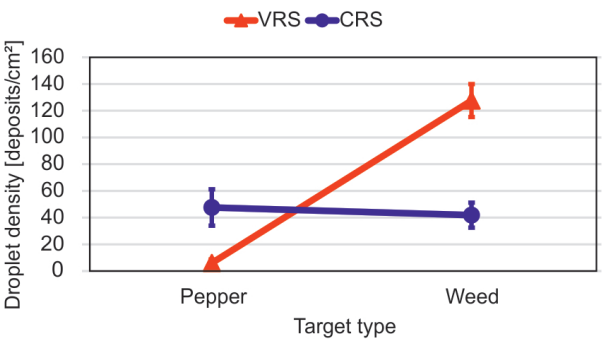


**Fig. 7.** The effect of the interaction between the sprayer type and target type on the droplet density

than VRS. The highest droplet density occurred with CRS at the speed of 3 km · h$^{-1}$. However, the VRS did not show a significant difference between the two studied speeds which both was higher than that of CRS at 2 km · h$^{-1}$ .

The interaction between the sprayer type and the target type showed a highly significant effect on the droplet density ($F_{1,56}$ = 25.5, $p < 10^{-7}$). Figure 7 demonstrates that the effect of the travel speed was more noticeable with CRS than VRS. The highest droplet density occurred with CRS at the speed of 3 km · h$^{-1}$. However, the VRS did not show a significant difference between the two studied speed which both was higher than that of CRS at 2 km · h$^{-1}$.

In relation to the sufficiency of the coverage of 40% to kill weed, this value was obtained under the spraying pressure of 3 bar. The required coverage is determined based on the type of herbicide used. Higher coverage is required to increase the efficacy of contact herbicides while it is not necessary with systemic herbicides (Marwan and Subr 2022; Shah *et al.* 2021). Therefore, if this percentage is not sufficient that may be fixed by increasing the spraying pressure.

## Weed detection and control evaluation

The results (Fig. 8) showed that all the losses started at low values and was decreasing till the end of the training. This indicates perfect performance of the model in differentiating between the weeds and the green peeper seedlings. Similarly, the results showed an increment of the mAP, precision, and recall values during the training. Moreover, the confusion matrix (Fig. 9) showed that all the weeds and the pepper seedlings were classified correctly.

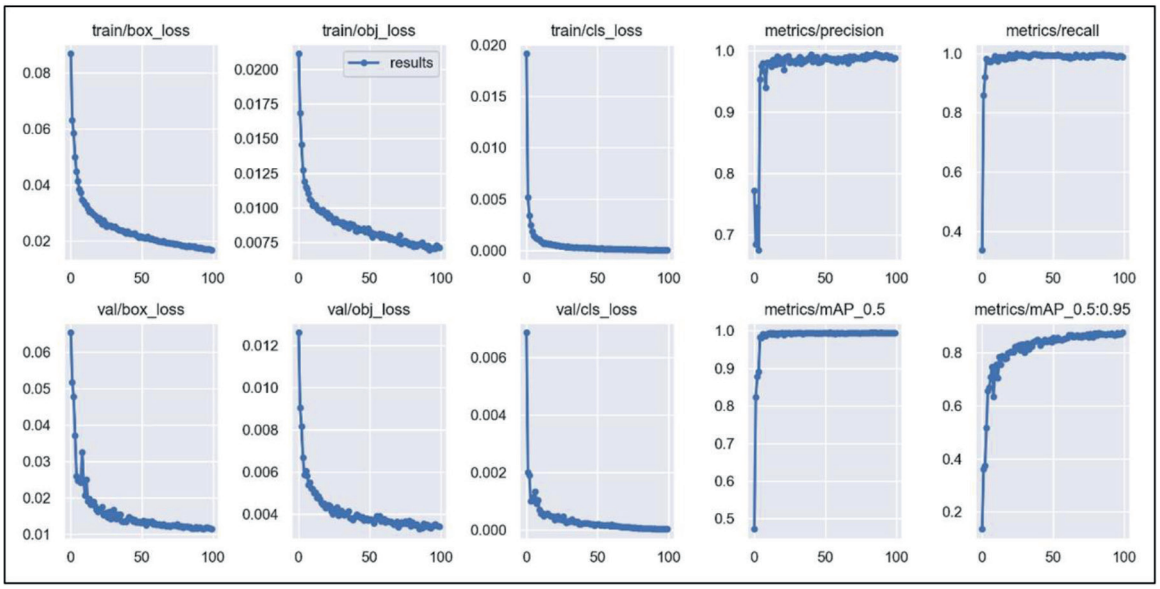


**Fig. 8.** Results of training the model (the x-axis refers to the epochs)

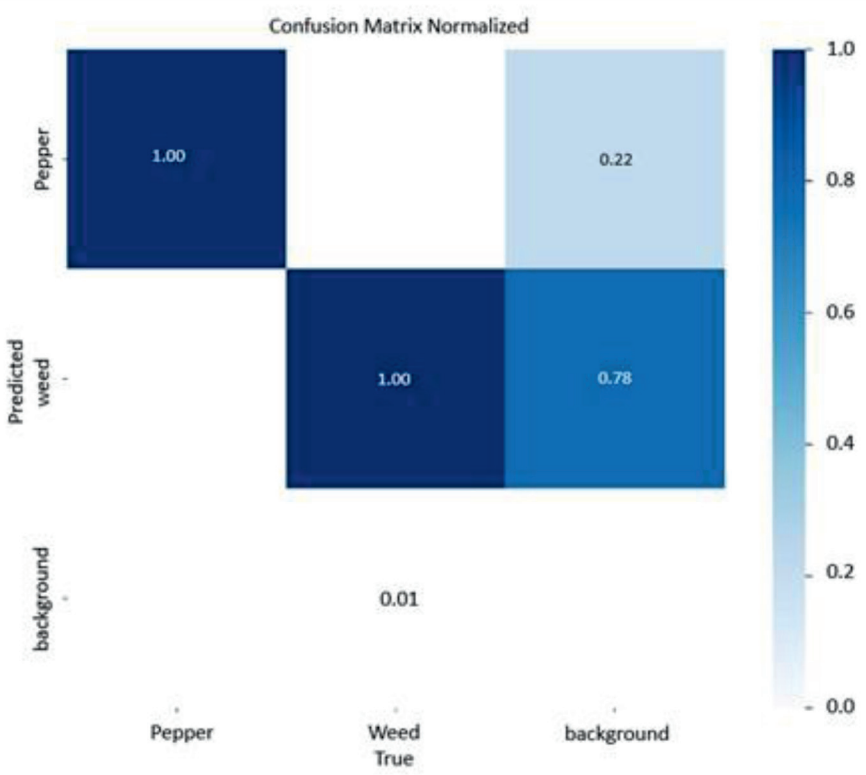


**Fig. 9.** Confusion matrix normalized

**Table 8.** Performance metrics of YOLOv5s for the studied classes

| Class | Images | Instances | Precision | Recall | mAP50 | Map50-95 |
|---|---|---|---|---|---|---|
| All | 170 | 261 | 0.982 | 0.994 | 0.994 | 0.887 |
| Pepper | 170 | 90 | 0.998 | 1 | 0.995 | 0.894 |
| Weed | 170 | 171 | 0.966 | 0.988 | 0.994 | 0.879 |

## Herbicide application evaluation

The precision, recall, accuracy, and error rate were measured based on the weed sprayed (true positive), the pepper not sprayed (true negative), the weed not sprayed (false negative), and the pepper sprayed (false positive). WSP (25 mm) were used to determine the sprayed and not sprayed objects. A coverage of 10% was considered as a threshold to determine the true positives and negatives and the false positives and negatives. Any plant that got a coverage less than 10% was considered a negative otherwise it was considered a positive.

The precision value which is one of the criteria that is usually used to measure the performance of the trained convolutional neural network such as YOLOv5. It specifically measures the proportion of the accurately predicted objects such as weed relative to all the predicted weeds including the accurately predicted weed and the pepper plants that were misclassified as weed, as we mentioned in equation 2 was calculated on the field (Fig. 10) and obviously indicated the superiority of the smart sprayer (AI) which achieved a precision of 90% at both travel speeds, whereas the

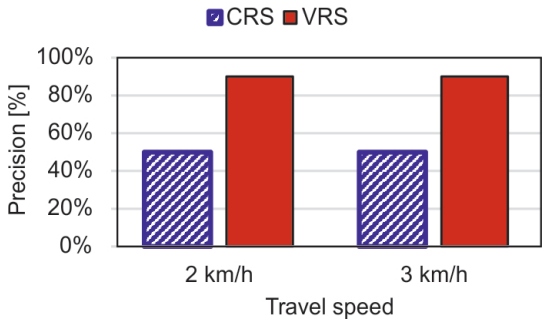


**Fig. 10.** The precision of applying herbicides for each of the two sprayers at the two selected travel speeds

remotely controlled sprayer (without smart prediction) and the conventional backpack sprayer achieved 50% as expected since all the pepper plants were sprayed as false positives.

The results of recall which is one of the criteria that is usually used to measure the performance of the trained convolutional neural network such as YOLOv5. It specifically measures the proportion of the accurately predicted objects such as weed relative to all the available actual weed including the accurately predicted weeds and the weeds that were missed to be classified as weed. As we mentioned in equation 3 that recall did not differ among the studied sprayers and achieved 100% for all sprayers (Fig. 11).

The results for accuracy shown in (Fig. 12) revealed a high accuracy of 94% for both studied speeds for the smart sprayer compared to 50% for the other two sprayers. This confirmed that smart sprayer successfully sprayed weeds and avoided spraying pepper to a high extent.

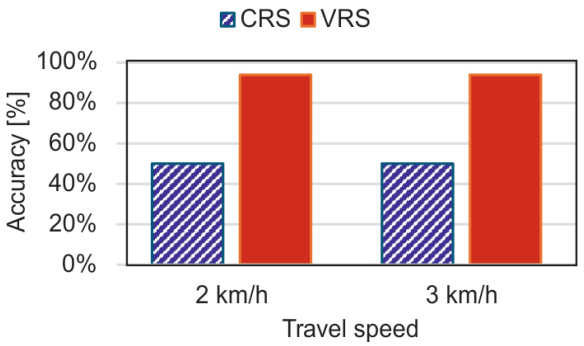


**Fig. 12.** The accuracy of applying herbicides for each of the two sprayers at the two selected travel speeds

The following two figures are supplementary figures that show the spray coverage and the droplet density at each treatment.

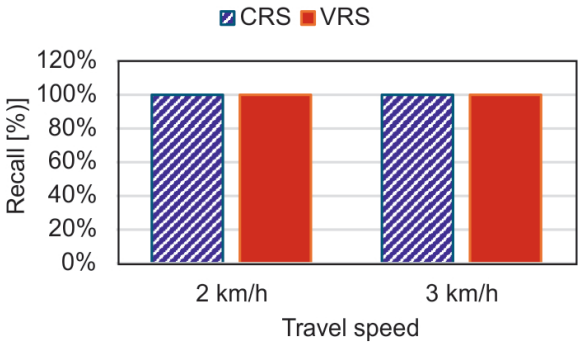


**Fig. 11.** The recall of applying herbicides for each of the two sprayers at the two selected travel speeds

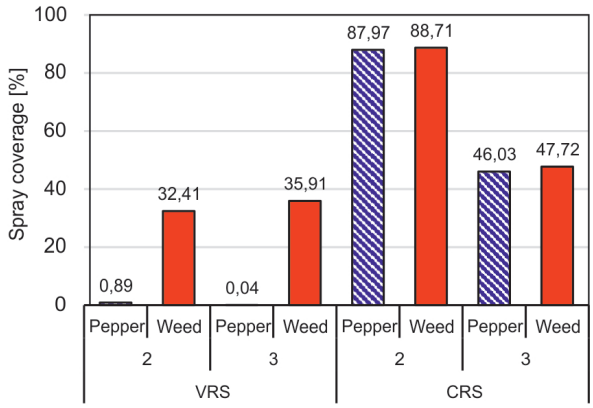


**Fig. 13.** The average of spray coverage at each treatment

**Table 9.** The true positives and negatives (greens), and the false positives and negatives (reds) for each treatment

| Sprayer type | Speed | Predicted Actual | Pepper | Weed | Total |
|---|---|---|---|---|---|
| CRS | 2 km · h$^{-1}$ | pepper | 0 | 9 | 9 |
| CRS | 2 km · h$^{-1}$ | weed | 0 | 9 | 9 |
| | | total | 0 | 18 | |
| CRS | 3 km · h$^{-1}$ | pepper | 0 | 9 | 9 |
| CRS | 3 km · h$^{-1}$ | weed | 0 | 9 | 9 |
| | | total | 0 | 18 | |
| VRS | 2 km · h$^{-1}$ | pepper | 8 | 1 | 9 |
| VRS | 2 km · h$^{-1}$ | weed | 0 | 9 | 9 |
| | | total | 8 | 10 | |
| VRS | 3 km · h$^{-1}$ | pepper | 8 | 1 | 9 |
| VRS | 3 km · h$^{-1}$ | weed | 0 | 9 | 9 |
| | | total | 8 | 10 | |

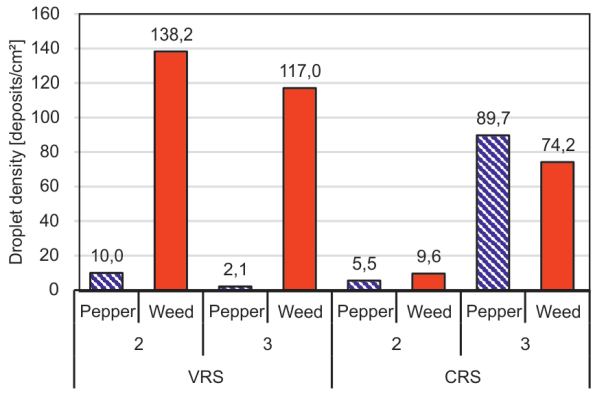


**Fig. 14.** The average of droplet density at each treatment

## Discussion

The difference in spray coverage between the VRS and the CRS was expected because for CRS, all the peppers and weeds were sprayed uniformly. In contrast, for VRS most of the peppers (non-target plants) were accurately recognized and were not sprayed and their coverage was near to zero, whereas almost all the weeds (target plants) were successfully sprayed that decreased the average of the spray coverage at the VRS. Although such an average may seem pointless at first glance, in our case it gives an indicator for how ignoring pepper by the VRS affects the average of the spray coverage because the coverage on the pepper was near to zero.

The results of the effect of travel speed on droplet density confirmed the findings of (Subr *et al.* 2020b) that increasing the travel speed increases the droplet density. However, the results obtained contradicted that of (Muhammad *et al.* 2019) which found that decreasing the flight speed of an airborne sprayer increased the droplet density. This may be attributed to the fact that the study of (Muhammad *et al.* 2019) used a UAV with the minimum speed of 7 at a height of 2 m which in turn may make the spray more susceptible to drift (Zhang *et al.* 2016) and evaporation at higher speed leading to lower droplet density. Whereas in our experiment the maximum speed and height were 3 and 50 cm, respectively, which makes the droplets less susceptible to the drift effect.

The results of the effect of the travel speed on the spray coverage confirmed that the spray coverage decreases with increasing the travel speed which agreed with the findings of (Qin *et al.* 2016; Hunter *et al.* 2020; Subr *et al.* 2020; Marwan and Subr 2022). It is known that the application rate decreases with the travel speed at a specific operating pressure which may in turn causes a decrease in the spray coverage. It is worth mentioning that the higher spray coverage does not necessarily leads to higher droplet density because the droplet density is the number of stains per unit area, therefore the lower the droplet size leads to higher droplet density and vice versa. However, the higher spray coverage may lead to droplets merging and then reduces the number of the droplets per unity area (droplet density).

The results of weed detection agreed with that of (Hussain *et al.* 2021a) who used YOLOv5s to differentiate between oak, grass, and wood which confirms the capability of YOLOv5s to predict objects at high level of accuracy, precision, and recall. The results of precision of herbicide application confirmed that the smart sprayer can be used successfully to avoid spraying the main plant especially when using non-selective herbicides that terminates the weeds as well as the plants. The results of recall of herbicide application confirmed that the smart sprayer did not miss any weed and can be used effectively as the other two sprayers which are not expected to miss any weed as well as pepper.

## Conclusions

This research confirms the potential of efficiently using the developed smart variable-rate sprayer for more sustainability to reduce costs and pollution. These results showed that the spray parameters such as the spray coverage, droplet density, and the deposition were less sensitive to travel speed when using the variable-rate sprayer. Moreover, the smart sprayer succeeded in reducing the amount of herbicide sprayed compared to the constant rate sprayer. The detection accuracy parameters were obviously higher in the variable-rate sprayer.

These results confirm the capability of the convolution neural network especially the custom trained YOLOv5s associated with a raspberry pi 4 computer connected with a co-processor (Coral USB accelerator) to be successfully used for real time applications such as weed detection and differentiating from the main crop since it provides reasonable and sufficient accuracy and inference time.

### References

Adamczewski K., Matysiak K., Kierzek R., Kaczmarek S. 2019. Significant increase of weed resistance to herbicides in Poland. Journal of Plant Protection Research 59 (2): 139–150. DOI: https://doi.org/10.24425/jppr.2019.129293

Al-Chalabi F.T., Hammood W.F. 2016a. Effect of integrated weed management on fiber quality characters of some cotton cultivars. Iraqi Journal of Agricultural Sciences 47 (1): 187–196. DOI: https://doi.org/10.36103/ijas.v47i1.620

Al-Chalabi F.T., Hammood W.F. 2016b. Response of growth analysis parameters of some cotton cultivars to integrated weed management. Iraqi Journal of Agricultural Sciences 47 (1): 197–207. DOI: https://doi.org/10.36103/ijas.v47i1.621

Al-Khafaji Mustafa.J., Safi S.M.A., Hammood W.F. 2023. Effect of herbicides on growth, grain yield and quality of barley. Iraqi Journal of Agricultural Sciences 54 (4): 1094–1100.

Al-khazali A.J., Shati R.K. 2016. Effect of some new herbicides on the competition ability to seven maize cultivars (*Zea mays* L. ) on the weed accompanying. Iraqi Journal of Agricultural Sciences 47 (2): 425–437. DOI: https://doi.org/10.36103/ijas.v47i2.585

Al-Mahmood A.M., Shahadi H.I., Khayeat A.R.H. 2022. Classifying Infected Palms with Dubas's Bug Based on Artificial Intelligence. p. 1–6. In: "International Conference on Electrical, Computer, and Energy Technologies, ICECET 2022". 20–22 July 2022, Prague, Czech Republic. DOI: https://doi.org/10.1109/ICECET55527.2022.9872955

Anon, n.d. YOLO v5 model architecture [Explained]. [Available on: https://iq.opengenus.org/yolov5/]. [Accessed on: 23 September 2023]

Aravind R., Daman M., Kariyappa B.S. 2016. Design and development of automatic weed detection and smart herbicide sprayer robot. p. 257–261. In: "2015 IEEE Recent Advances in Intelligent Computational Systems, RAICS 2015". 2016. DOI: https://doi.org/10.1109/RAICS.2015.7488424

Bakhshipour A., Jafari A. 2018. Evaluation of support vector machine and artificial neural networks in weed detection using shape features. Computers and Electronics in Agriculture 145: 153–160. DOI: https://doi.org/10.1016/j.compag.2017.12.032

Chandel N.S., Chakraborty S.K., Rajwade Y.A., Dubey K., Tiwari M.K., Jat D. 2021. Identifying crop water stress using deep learning models. Neural Computing and Applications 33 (10): 5353–5367. DOI: https://doi.org/10.1007/s00521-020-05325-4

Coleman G., Salter W., Walsh M. 2022. Open Weed Locator (OWL): an open-source, low-cost device for fallow weed detection. Scientific Reports 12 (1): 1–12. DOI: https://doi.org/10.1038/s41598-021-03858-9

Cunha M., Carvalho C., Marcal A.R.S. 2012. Assessing the ability of image processing software to analyse spray quality on water-sensitive papers used as artificial targets. Biosystems Engineering 111 (1): 11–23. DOI: https://doi.org/10.1016/j.biosystemseng.2011.10.002

Dian Bah M., Hafiane A., Canals R. 2018. Deep learning with unsupervised data labeling for weed detection in line crops in UAV images. Remote Sensing 10 (11): 1690. DOI: https://doi.org/10.3390/rs10111690

Farooque A.A., Hussain N., Schumann A.W., Abbas F., Afzaal H., McKenzie-Gopsill A., Esau T., Zaman Q., Wang X. 2023. Field evaluation of a deep learning-based smart variable-rate sprayer for targeted application of agrochemicals. Smart Agricultural Technology 3: 100073.

Ferguson J.C., Chechetto R.G., Hewitt A.J., Chauhan B.S., Adkins S.W., Kruger G.R., O'Donnell C.C. 2016. Assessing the deposition and canopy penetration of nozzles with different spray qualities in an oat (Avena sativa L.) canopy. Crop Protection 81: 14–19. DOI: https://doi.org/10.1016/j.cropro.2015.11.013

Ghadi N.M., Salman N.H. 2022. Deep Learning-Based Segmentation and Classification Techniques for Brain Tumor MRI: A Review. Journal of Engineering 28 (12): 93–112. DOI: https://doi.org/10.31026/j.eng.2022.12.07

Hunter J.E., Gannon T.W., Richardson R.J., Yelverton F.H., Leon R.G. 2020. Coverage and drift potential associated with nozzle and speed selection for herbicide applications using an unmanned aerial sprayer. Weed Technology 34 (2): 235–240. DOI: https://doi.org/10.1017/wet.2019.101

Hussain A., Barua B., Osman A., Abozariba R., Asyhari A.T. 2021a. Low Latency and Non-Intrusive Accurate Object Detection in Forests. p. 1–6. In: "2021 IEEE Symposium Series on Computational Intelligence, SSCI 2021 – Proceedings." 2021. DOI: https://doi.org/10.1109/SSCI50451.2021.9660175

Hussain N., Farooque A.A., Schumann A.W., Abbas F., Acharya B., McKenzie-Gopsill A., Barrett R., Afzaal H., Zaman Q.U., Cheema M.J.M. 2021b. Application of deep learning to detect Lamb's quarters (Chenopodium album L.) in potato fields of Atlantic Canada. Computers and Electronics in Agriculture 182: 106040. DOI: https://doi.org/10.1016/j.compag.2021.106040

Idziak R., Waligóra H., Szuba V. 2022. The influence of agronomical and chemical weed control on weeds of corn. Journal of Plant Protection Research 62 (2): 215–222. DOI: https://doi.org/10.24425/jppr.2022.141362

Konar J., Khandelwal P., Tripathi R. 2020. Comparison of Various Learning Rate Scheduling Techniques on Convolutional Neural Network. p. 1–5. In: "2020 IEEE International Students' Conference on Electrical, Electronics and Computer Science, SCEECS". 22–23 Feb. 2020, Bhopal, India. DOI: https://doi.org/10.1109/SCEECS48394.2020.94

Kulkarni S., Angadi S.A., Belagavi V.T.U. 2019. IoT based weed detection using image processing and CNN. International Journal of Engineering Applied Sciences and Technology 4 (3): 606–609.

Marangoni Junior A., da Costa Ferreira M. 2019. Influence of working pressure and spray nozzle on the distribution of spray liquid in manual backpack sprayers. Arquivos do Instituto Biológico 86: 1–9. DOI: https://doi.org/10.1590/1808-1657000442018

Marwan I., Subr A. 2022. Developing and testing of automated sprayer for agrochemicals application trials in Iraq. Muthanna Journal for Agricultural Sciences 9 (1): 10–24. DOI: https://doi.org/10.52113/mjas04/9.1/2

Milanowski M., Subr A., Combrzyński M., Różańska-Boczula M., Parafiniuk S. 2022. Effect of adjuvant, concentration and water type on the droplet size characteristics in agricultural nozzles. Applied Sciences (Switzerland) 12 (12): 5821. DOI: https://doi.org/10.3390/app12125821

Muhammad M.N., Wayayok A., Mohamed Shariff A.R., Abdullah A.F., Husin E.M. 2019. Droplet deposition density of organic liquid fertilizer at low altitude UAV aerial spraying in rice cultivation. Computers and Electronics in Agriculture 167: 105045. DOI: https://doi.org/10.1016/j.compag.2019.105045

Nyarko B.N.E., Bin W., Jinzhi Z., Odoom J. 2023. Tomato fruit disease detection based on improved single shot detection algorithm. Journal of Plant Protection Research 63 (4): 405–417. DOI: https://doi.org/10.24425/jppr.2023.146877

Pannacci E., Bartolini S. 2018. Evaluation of chemical weed control strategies in biomass sorghum. Journal of Plant Protection Research 58 (4): 404–412. DOI: https://doi.org/10.24425/jppr.2018.125881

Parafiniuk S., Milanowski M., Subr A.K. 2015. The influence of the water quality on the droplet spectrum produced by agricultural nozzles. Agriculture and Agricultural Science Procedia 7: 203–208. DOI: https://doi.org/10.1016/j.aaspro.2015.12.018

Parafiniuk S., Milanowski M., Subr A., Krawczuk A. 2017. Influence of surface tension of water on droplet size produced by flat jet nozzles: 295–300. DOI: https://doi.org/10.24326/fmpmsa.2017.53

Partel V., Charan Kakarla S., Ampatzidis Y. 2019a. Development and evaluation of a low-cost and smart technology for precision weed management utilizing artificial intelligence. Computers and Electronics in Agriculture 157: 339–350. DOI: https://doi.org/10.1016/j.compag.2018.12.048

Partel V., Kim J., Costa L., Pardalos P., Ampatzidis Y. 2019b. Smart Sprayer for Precision Weed Control Using Artificial Intelligence: Comparison of Deep Learning Frameworks. ISAIM (pp. 101-105).

Qin W.C., Qiu B.J., Xue X.Y., Chen C., Xu Z.F., Zhou Q.Q. 2016. Droplet deposition and control effect of insecticides sprayed with an unmanned aerial vehicle against plant hoppers. Crop Protection 85: 79–88. DOI: https://doi.org/10.1016/j.cropro.2016.03.018

Shah T.M., Nasika D.P.B., Otterpohl R. 2021. Plant and weed identifier robot as an agroecological tool using artificial neural networks for image identification. Agriculture (Switzerland) 11 (3): 222. DOI: https://doi.org/10.3390/agriculture11030222

Subeesh A., Bhole S., Singh K., Chandel N.S., Rajwade Y.A., Rao K.V.R., Kumar S.P., Jat D. 2022. Deep convolutional neural network models for weed detection in polyhouse grown bell peppers. Artificial Intelligence in Agriculture 6: 47–54. DOI: https://doi.org/10.1016/j.aiia.2022.01.002

Subr A., Al-Ahmadi A., Abbas M. 2020. Effect of nozzle type and some locally used surfactants on the spray quality. Iraqi Journal of Agricultural Sciences 51 (3): 856–864. DOI: https://doi.org/10.36103/ijas.v51i3.1040

Subr A., Parafiniuk S., Milanowski M., Krawczuk A., Kachel M. 2020a. Study of deposited spray quality of spraying agents with different physical properties. Plant Archives 20 (2): 6109–6114.

Subr A., Parafiniuk S., Milanowski M., Krawczuk A., Kachel M. 2020b. Study of deposited spray quality of spraying agents with different physical properties. Plant Archives 20 (2): 6109–6114.

Sujaritha M., Annadurai S., Satheeshkumar J., Kowshik Sharan S., Mahesh L. 2017. Weed detecting robot in sugarcane fields using fuzzy real time classifier. Computers and Electronics in Agriculture 134: 160–171. DOI: https://doi.org/10.1016/j.compag.2017.01.008

Urmashev B., Buribayev Z., Amirgaliyeva Z., Ataniyazova A., Zhassuzak M., Turegali A. 2021. Development of a weed detection system using machine learning and neural network algorithms. Eastern-European Journal of Enterprise Technologies 6 (2): 70–85. DOI: https://doi.org/10.15587/1729-4061.2021.246706

Veisi M., Zand E., Moeini M.M., Bassiri K. 2020. Review of research on weed management of chickpea in Iran: Challenges, strategies and perspectives. Journal of Plant Protection Research 60 (2): 113–125. DOI: https://doi.org/10.24425/jppr.2020.132212

Villette S., Maillot T., Guillemin J.P., Douzals J.P. 2021. Simulation-aided study of herbicide patch spraying: Influence of spraying features and weed spatial distributions. Computers and Electronics in Agriculture 182: 105981. DOI: https://doi.org/10.1016/j.compag.2020.105981

Wang P., Tang Y., Luo F., Wang L., Li C., Niu Q., Li H. 2022. Weed25: A deep learning dataset for weed identification. Frontiers in Plant Science 13: 1053329. DOI: https://doi.org/10.3389/fpls.2022.1053329

Zhang P., Deng L., Lyu Q., He S.L., Yi S.L., De Liu Y., Yu Y.X., Pan H.Y. 2016. Effects of citrus tree-shape and spraying height of small unmanned aerial vehicle on droplet distribution. International Journal of Agricultural and Biological Engineering 9 (4): 45–52. DOI: https://doi.org/10.3965/j.ijabe.20160904.2178

Zhu H., Liu H., Shen Y., Liu H., Zondag R.H. 2017. Spray deposition inside multiple-row nursery trees with a laser-guided sprayer. Journal of Environmental Horticulture 35 (1): 13–23. DOI: https://doi.org/10.24266/0738-2898-35.1.13

Zhu H., Salyani M., Fox R.D. 2011. A portable scanning system for evaluation of spray deposit distribution. Computers and Electronics in Agriculture 76 (1): 38–43. DOI: https://doi.org/10.1016/j.compag.2011.01.003